Constraint-Based Control of a Distally Actuated Continuum Robot*

Beatriz Farola Barata[1,2], Gianni Borghesan[1,3], Diego Dall'Alba[2], Jos Vander Sloten[1], and Emmanuel Vander Poorten [1]

[1] *Robot-Assisted Surgery Group, Department of Mechanical Engineering, KU Leuven, Belgium*
[2] *Altair Robotics Laboratory, Department of Computer Science, University of Verona, Italy*
[3] *Core Lab ROB, Flanders Make, Belgium*
beatriz.barata@kuleuven.be

INTRODUCTION

Endovascular catheterization is a minimally invasive procedure typically carried out with the use of catheters, inserted in the vasculature and steered towards a desired site. Preventing damage to the vasculature relies on the precise navigation of the catheter's tip, while minimizing the contact between the instrument and the vasculature [1]. Robotic technology is increasingly investigated in such task, as it promises a high level of precision. Robots could further perform complex coordinated motion in 3D space. Developing a safe and precise controller that accounts for the large amount of variability is far from trivial. In order to tackle the associated challenges, different control approaches have been introduced, such as multi-task control frameworks [2].

This work proposes a constraint-based velocity-resolved control approach for a steerable catheter, with a distal bending segment. Figure 1 shows the steerable catheter with distal bending segment (in red) between the base $\mathbf{p}_b$ and the tip $\mathbf{p}_t$ of the catheter. The controller is tested inside a virtual aortic vessel model.

Given the vessel centerline, locally approximated as a line cl, the controller is designed such that the catheter tip navigates within a safe zone (defined by a safe distance $\mathbf{d}_s$) around cl; and the mid-node of the bending segment backbone $\mathbf{p}_n$ (situated between $\mathbf{p}_t$ and $\mathbf{p}_b$) keeps minimal contact with the vessel wall. The goal of this work is to propose and assess a control framework for the aforementioned control problem.

MATERIALS AND METHODS

The robot is controlled with a velocity-resolved constraint-based scheme [3]. This kind of approach requires the following elements: *i)* a forward kinematic and differential forward kinematic functions relating the actuator space and task space, *ii)* control equations solved with a quadratic programming (QP) approach, and *iii)* task specification. The kinematic relation between $\mathbf{y}$ (output space) and $\mathbf{q}$ (actuator space) and the obtained control actions (based on the generalized Jacobian matrix $\mathbf{J}$) are described as follows:

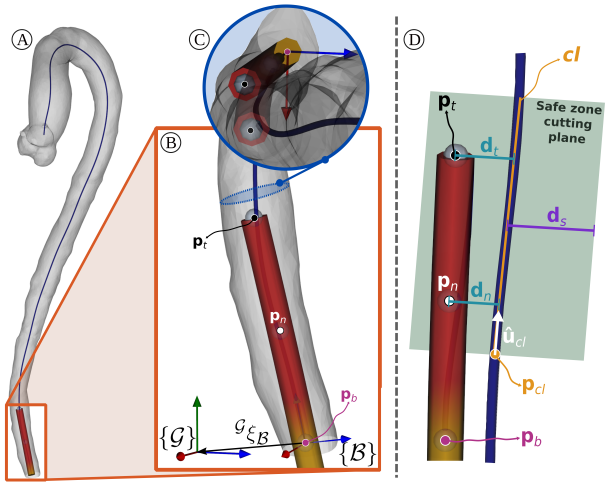

Figure 1: System's overview in the simulated aortic model (A), with a focus on the different components of the robot and relevant frames in (B). Representations of the control outcome in the xy plane ((C)) and of the overall control approach with relevant variables ((D)) are shown.

$$\mathbf{y} = \mathbf{g}(\mathbf{q}), \qquad \dot{\mathbf{y}} = \mathbf{J}(\mathbf{q})\dot{\mathbf{q}} = \frac{\partial\, \mathbf{g}(\mathbf{q})}{\partial\, \mathbf{q}}\, \dot{\mathbf{q}} \tag{1}$$

In our case, position and velocity constraints (*i.e.* task functions) are defined. A velocity constraint imposes that a particular velocity is followed by the time derivative of an expression $\mathbf{g}(\mathbf{q})$. Desired velocities $\dot{\mathbf{y}}_d^o$ are computed as:

$$\dot{\mathbf{y}}_d^o = \mathbf{K}_p(\mathbf{y}_d - \mathbf{y}) \tag{2}$$

where $(\mathbf{y}_d - \mathbf{y}) = e$ (error) and $\mathbf{y}_d$ and $\mathbf{y}$ represent the desired and measured positions, respectively. $\mathbf{K}_p$ (dimensions: $[1/s]$) are the gains of the controller. A similar reasoning can be applied to inequalities, see [3].

*This work was supported by the ATLAS project. The ATLAS project has received funding from the European Union's Horizon 2020 research and innovation programme under the Marie Sklodowska-Curie grant agreement No 813782.

Forward and differential kinematics: The task spatial relation is described by two mapping functions, the robot kinematics (cc), and the distance function (dst). These, combined and differentiated, provide the kinematics in function of ($\mathbf{q}$):

$$\mathbf{d} = \mathbf{g}_{dst}(\mathbf{g}_{cc}) \tag{3}$$

$$\mathbf{J}(\mathbf{q}) = \mathbf{J}_{dst}(\mathbf{p}_c)\ \mathbf{J}_{cc}(\mathbf{q}) \tag{4}$$

where $\mathbf{J}$ is the task Jacobian matrix, and $\mathbf{p}_c$ denotes any node on the robot's bending segment backbone.

The catheter has three control variables $\mathbf{q}$ from its three degrees of freedom (DoFs): the bending angle θ, the bending direction angle ϕ of the distal segment, and the insertion ρ.

$\mathbf{g}_{cc}(\mathbf{q})$ is characterized as the constant curvature kinematics (no external loads assumed), further discussed in [4]. The catheter's bending segment is thus modeled as a circular arc, with l as the arc length:

$$\mathbf{g}_{cc}(\mathbf{q}) = {}^{\mathcal{G}}\xi_{\mathcal{B}} \begin{bmatrix} \frac{l cos\phi\,(1-cos\,\theta)}{\theta} \\ \frac{l sin\phi\,(1-cos\,\theta)}{\theta} \\ \frac{l cos\,\theta}{\theta} \end{bmatrix} \tag{5}$$

${}^{\mathcal{G}}\xi_{\mathcal{B}}$ denotes the orientation of frame $\{\mathcal{B}\}$, attached to the base ($\mathbf{p}_b$) of the bending segment and in which the constant curvature kinematics are determined, with respect to the global reference frame $\{\mathcal{G}\}$ (see fig. 1).

$\mathbf{g}_{dst}$ is the task-specific function mapping, formulated as follows:

$$\mathbf{g}_{dst}(\mathbf{p}_c) = \frac{\|(\mathbf{p}_c - \mathbf{p}_{cl}) \times \hat{\mathbf{u}}_{cl}\|}{\|\hat{\mathbf{u}}_{cl}\|} \tag{6}$$

where all elements are expressed in the global frame $\{\mathcal{G}\}$ with $\mathbf{p}_{cl}$ being a point on the approximated centerline cl and $\hat{\mathbf{u}}_{cl}$ its direction vector ($cl = \mathbf{p}_{cl} + \hat{\mathbf{u}}_{cl}\, t,\ t \in \mathbb{R}$).

QP-based continuum robot control strategy: A QP optimization problem is formulated for deriving the control variables velocities $\dot{\mathbf{q}}$ from desired output variations, considering different task functions:

$$\underset{\mathbf{x}}{\text{minimize}} \qquad \mathbf{x}^T\mathbf{H}\mathbf{x} \tag{7a}$$

$$\text{subject to} \qquad \mathbf{L}_b \leq \mathbf{A}\mathbf{x} \leq \mathbf{U}_b \tag{7b}$$

$$\mathbf{l}_b \leq \mathbf{x} \leq \mathbf{u}_b \tag{7c}$$

where $\mathbf{x}$ denotes the vector $[\dot{\mathbf{q}} \quad \varepsilon]$ (ε is a vector of slack variables). $\mathbf{H}$ is a diagonal matrix comprising both the control variables and the slack variables weights [3]. From eq. (1) and eq. (2), the robot's tasks, relative to the tip and mid-node (with their respective Jacobian matrices), are implemented in the QP algorithm (eq. (7b)) as position constraints (frame $\{\mathcal{G}\}$):

$$\mathbf{J}(\mathbf{q})\,\dot{\mathbf{q}} \sim \mathbf{K}_p\, e + \varepsilon \quad \text{where} \quad \sim \in \{=, \leq, \geq\} \tag{8}$$

Task specification using constraints: Three position and one velocity constraints, detailed in Table 1, are enforced so the catheter tip navigates in a user-defined safe zone while minimizing contact between the vessel and the catheter body.

Table 1: Implemented constraints overview. Note that constraints are divided into two priority levels: hard (higher priority) and soft (lower priority) [3].

# Constraint	Type	Target
1 – Tip safety	Hard inequality	$\mathbf{g}_{dst}(\mathbf{p}_t) \leq 6$ [mm]
2 –Tip towards centerline	Soft equality	$\mathbf{g}_{dst}(\mathbf{p}_t) = 0$ [mm]
3 – Mid-node towards centerline	Soft equality	$\mathbf{g}_{dst}(\mathbf{p}_n) = 0$ [mm]
4 – Forward insertion	Soft inequality	$\dot{\boldsymbol{\rho}} \geq 1$ [mm/step]

Experiment: From the task specification, an experiment was carried out in which, during insertion, the measured distances, $\mathbf{d}_t$ and $\mathbf{d}_n$, of the catheter tip and mid-node from the centerline were recorded. Constraints 2, 3 and 4 (soft constraints) were given weighting factors of 0.6, 0.7 and 0.5, respectively.

RESULTS

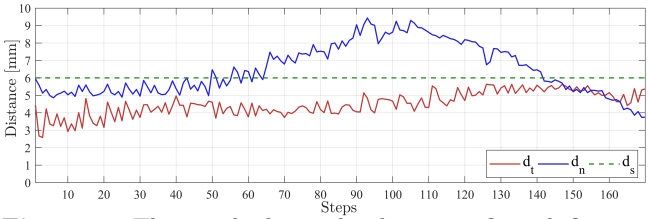

Figure 2: The graph shows the distances $\mathbf{d}_t$ and $\mathbf{d}_n$ as a function of the simulation steps considering the task specification. $\mathbf{d}_s$ depicts the safe zone distance for the catheter's tip. The obtained results are relative to the initial section of the aortic model.

CONCLUSION AND DISCUSSION

Overall, the controller demonstrated safe navigation and minimal contact between the vessel and the robot. The catheter tip was kept within the safe zone and the mid node of its distal segment showed no contact with the simulated environment (the aortic model is considered to have a radius of 16 mm). Having one active segment leads to a trade-off: one node's convergence to the centerline often translates into the other's divergence (fig. 2). The proposed task specification was successfully verified.

REFERENCES

[1] E. Rijanto, A. Sugiharto, S. Utomo, R. Rahmayanti, H. Afrisal, and T. Nanayakkara, "Trends in robot assisted endovascular catheterization technology: A review," in *2017 International Conference on Robotics, Biomimetics, and Intelligent Computational Systems (Robionetics)*, 2017, pp. 34–41.

[2] M. T. Chikhaoui and J. Burgner-Kahrs, "Control of continuum robots for medical applications: State of the art," in *ACTUATOR 2018; 16th International Conference on New Actuators*, 2018, pp. 1–11.

[3] E. Aertbeliën and J. De Schutter, "Etasl/etc: A constraint-based task specification language and robot controller using expression graphs," in *2014 IEEE/RSJ International Conference on Intelligent Robots and Systems*, 2014, pp. 1540–1546.

[4] T. Mahl, A. Hildebrandt, and O. Sawodny, "A variable curvature continuum kinematics for kinematic control of the bionic handling assistant," *IEEE Transactions on Robotics*, vol. 30, no. 4, pp. 935–949, 2014.